MAGNETIC FIELD ANALYSIS FOR A RELUCTANCE SYNCHRONOUS MACHINE

I.A. VIOREL[1] - I. HUSAIN[2] - IOANA CHIŞU[1] - H.C. HEDEŞIU[1] - K.Á. BIRÓ[1] - L. SZABÓ[1]

[1] Dept. of Electrical Machines, Technical University of Cluj-Napoca
Daicoviciu 15, RO-3400 Cluj-Napoca, Romania
phone: +40 64 195 699 – fax: +40 64 192 055; e-mail: Ioan.Adrian.Viorel@mae.utcluj.ro

[2] University of Akron, Dept. of Electrical Engineering
Akron, OH 44325-3904, USA
e-mail: ihusain@uakron.edu

ABSTRACT

Reluctance synchronous motor (RSM) can be an alternative to field oriented induction motor. The RSM's rotor topology is the key of the problem since an important saliency ratio leads to high power factor, torque/ampere and constant power speed range. This paper analyses a segmental rotor topology for a four pole RSM with concentrated nonmagnetic materials and flux barriers to reduce the q-axis flux.

1. INTRODUCTION

The reluctance synchronous motor (RSM) is a singly salient machine. Its rotor is built up to employ the principle of reluctance torque to produce electromechanical energy conversion. As proved in previously published scientific works, good synthesises are given in [1], [2], RSMs are very attractive for line-start and variable speed electric drives. Their torque density, power factor and efficiency are competitive if the saliency ratio is high. The RSMs also offer fast torque and speed dynamics and wide speed range operation.

Almost all of the RSM's important performance parameters depends on the synchronous inductance ratio, or saliency ratio, K=Ld/Lq. The RSM's rotor is the most important key factor in obtaining the high saliency ratio. It emerged different RSM rotor constructions, the most important being [1]-[3]:

1. Segmental rotors
2. Rotors with flux guides and flux barriers
3. Axially laminated rotors

The literature consistently shows that the axially laminated rotors without starting cage produce the highest saliency ratio, [1]-[4]. The multiple barrier rotors with flux guides, which behaves almost as the axially laminated rotors, offer the possibility to achieve important saliency ratio too, (K=7÷11, [3]). Both these topologies imply quite complicated technology and high costs. Such a RSM may cost more than an equivalent induction motor (IM) and it should compensate the cost by its performances. There are a number of possible applications for RSM where the cost of the drive is of major importance. In such a case, a non-optimal structure may be chosen in favour of simpler and cheaper construction. From this point of view the rotor topology is the

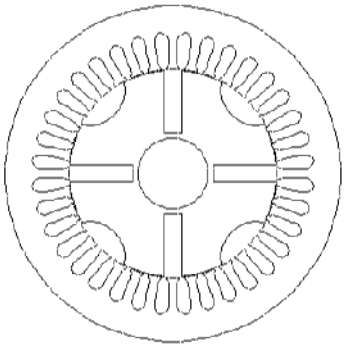

Fig. 1. Motor structure

most important, since, as usually, the stator core is the same as for an induction motor and comes from a mass production, being of quite low cost.

The segmental and single flux barrier rotors are the simplest topologies for the cageless RSM, and they allow for a saliency ratio between 3.5 and 6, the greater values corresponding to large motors [2], [3]. The chosen topology was a segmental rotor with concentrated nonmagnetic material, Fig. 1. Such a topology was previously proposed for a two pole RSM [5], but it implied technological difficulties, which can be partially avoided in the four pole case. The four pole rotor magnetic core was made of crude induction motor magnetic sheets manufactured to the actual topology. The prototype was built up using the stator core and the case of a 5.5 kW induction motor, the stator winding remaining unchanged. In the design stage different rotor topologies were considered. The chosen one allows for the highest saliency ratio with a less complicated structure and air-gap harmonics content. The MagNet software package was used for 2D FEM analysis.

2. FEM ANALYSIS RESULTS AND CONCLUSIONS

Taking into account the results obtained in [5] and the technological difficulties, which the two pole rotor implies, the solution considered was quite the same, but for a four poles motor. Basically, the solution remains a segmental rotor with concentrated nonmagnetic material, Fig.1.

In the designing stage, many variants were tested via 2D FEM magnetic field computation. The stator remains unchanged since it is an induction motor stator with 36 slots and a double layer winding. In Fig. 2 the flux plots on the d and q-axis are presented for some of the variants, the phase current being 12.4 A.

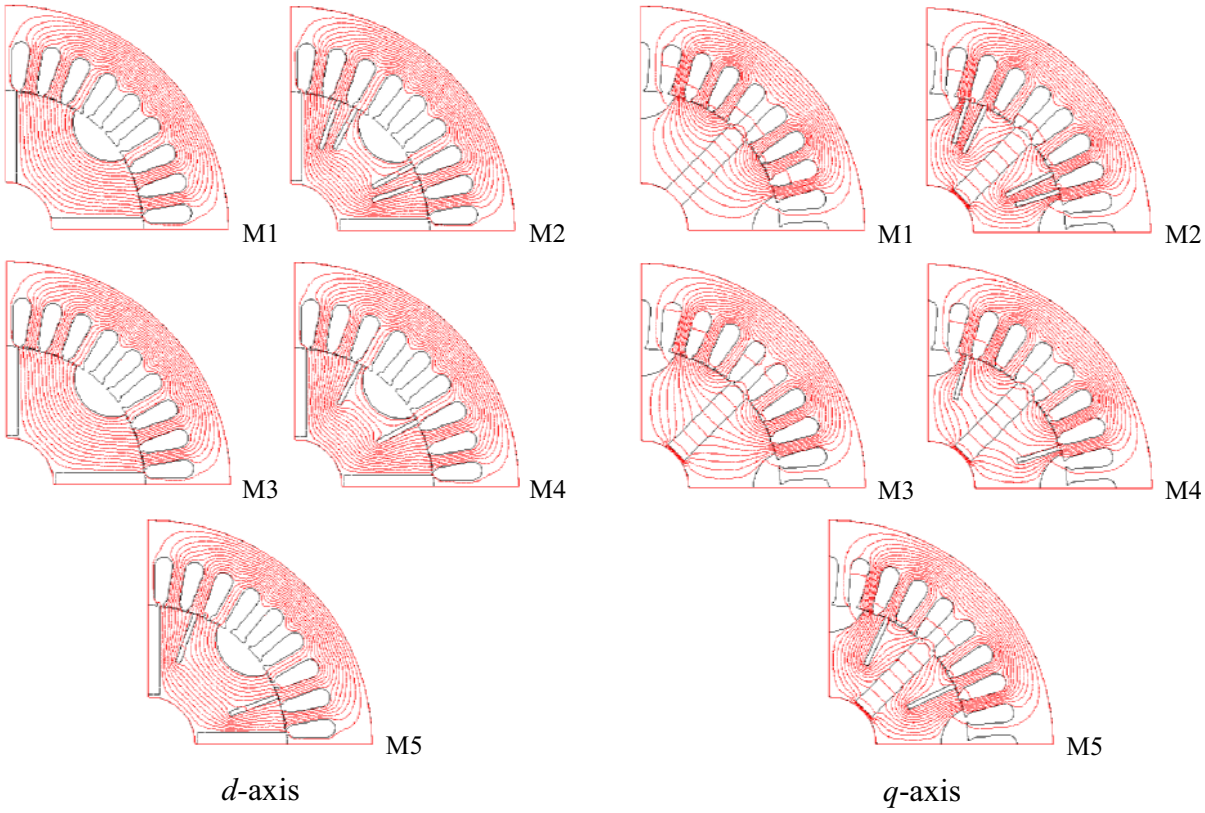

Fig. 2. The *d*- and *q*-axis flux plots for M1-M5 rotor variants

All the variants given in Fig. 2 have the concentrated nonmagnetic material on the rotor d-axis with a width of 10 mm and the semicircular slot with the minimum radius on the q-axis. The ideal variant, M1, has no core bridge between the rotor segments and no flux barriers.

For variants M2-M5, given in Fig. 2, the semicircular slot has the same radius, but there is a 2 mm core bridge between rotor segments. For M2 variant two radial flux barriers were considered since M4 and M5 have respectively only one of the barriers. The M3 variant is identical to M1 one, but it has core bridge between rotor segments.

The values of the magnetising inductances, M_d, M_q, the saliency ratio $K=M_d/M_q$, the electromagnetic torque T, and efficiency η for M1-M5 variants computed via the 2D FEM analysis, are given in Table I.

Table I

	M_d [mH]	M_q [mH]	K	T [Nm]	η
M1	116,329	19,866	5.855	19.3	0.735
M2	109,893	27,143	4.048	18.0	0.721
M3	116,323	28,050	4.146	19.4	0.736
M4	112,945	27,486	4.109	18.7	0.728
M5	113,502	27,748	4.090	18.8	0.729

The electromagnetic torque is:

$$T = p(L_d - L_q) I_d^2 \frac{1}{k} \tag{1}$$

where

$$k = \frac{I_d}{I_q} = \frac{\lambda_d}{\lambda_q} \frac{L_q}{L_d} \tag{2}$$

and the synchronous inductances are

$$L_d = M_d + L_{s\sigma}; \quad L_q = M_q + L_{s\sigma} \tag{3}$$

$L_{S\sigma}$ being the stator phase leakage inductance. The efficiency comes as:

$$\eta = \frac{P_2}{P_2 + \Sigma p} \cong \frac{T\Omega_s}{T\Omega_s + \Sigma p} \tag{4}$$

where $\Omega_s = 2\pi n_s = 157.08$ rad/sec ; $\Sigma p = p_{js} + p_{Fe} + p_m$; $p_{js} = 3R_s \cdot I_s^2$

The iron core losses, p_{Fe}, and the mechanical losses, p_m, were taken equal to the computed losses of the corresponding induction motor, p_{Fe}=205 W, p_m=22 W.

The stator phase leakage inductance $L_{S\sigma}$ is computed as usually [6], the value, which includes the end winding leakage, being $L_{S\sigma}$=8.5256 mH.

The parameters to vary in order to obtain the different rotor variants analysed via 2D FEM were: the nonmagnetic material width (2 mm step being considered) the radius of the semicircular slot, and the depth of the radial flux barriers. As one can see, the influence of the flux barriers is not useful since the presence of the flux barrier slightly decreases the q-axis magnetising inductance,

but reduces more the d-axis magnetising inductance. The semicircular hole on the q-axis does not lead to an important saliency ratio increase, but this hole had to be kept due to technological reasons since the rotor structure is consolidated with four insulated nonmagnetic bars placed in that holes. The bars are belted together with special rings, made of nonmagnetic insulated material, fixed on the shaft outside the rotor's stack.

The core bridge between the rotor segments does not affect the d-axis magnetising inductance, as one can see comparing the M1 and M3 models. The q-axis magnetising inductance is increased with 34% and consequently decreases the saliency ratio K. The rotor shaft is of nonmagnetic material and it was adequately considered in the 2D FEM model.

The harmonic content of the air-gap field is quite important and it can be seen from the harmonic analysis done. The results of this analysis for the *d*-axis air-gap field for the M3 model are shown in Fig. 3. In this figure the air-gap flux density variation on a pole pitch and the corresponding harmonic analysis is shown for the case of the stator MMF oriented on the rotor *d*-axis direction.

The overall conclusion is that the segmental rotor topology proposed here is a very simple one, and allows for achieving quite good performance, the ratio cost / performance being a very good one.

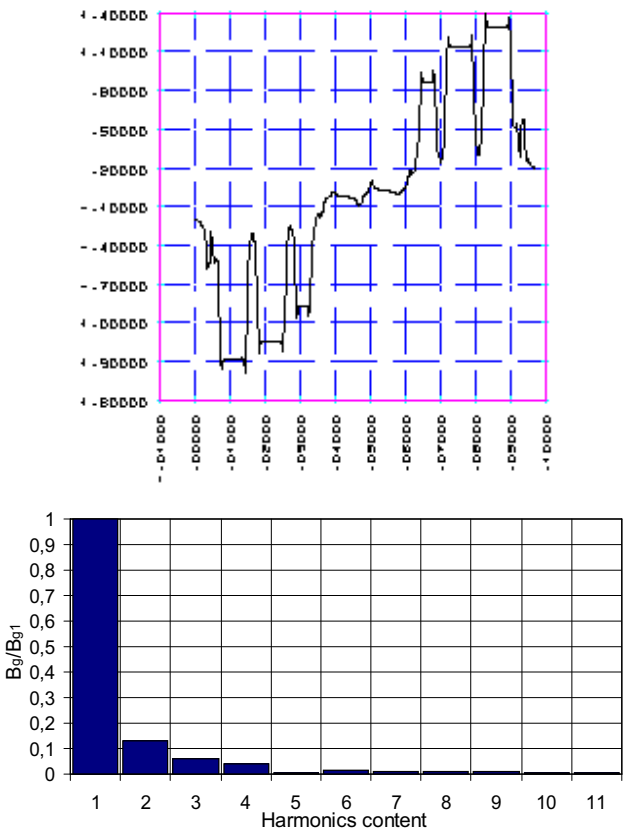

Fig. 3. The air-gap flux density variation on a pole pitch and the corresponding harmonic spectrum for *d*-axis

3. REFERENCES

[1] Boldea, *Reluctance synchronous machines and drives*, Clarendon Press, Oxford (1996).

[2] G. Henneberger, I.A. Viorel, *Variable reluctance electrical machines*, Shaker Verlag, Aachen (2001).

[3] D.A. Staton, T.J.E. Miller, S.E. Wood, "Maximising the saliency ratio of the synchronous reluctance motor", *IEE Proc.-B*, Vol. 140, No. 4, pp. 249-259, July 1993.

[4] T. Matsuo, T.A. Lipo, "Rotor design optimization of synchronous reluctance machine", *IEEE Transactions on Energy Conversion*, Vol. 9, No. 2, pp. 359-365, June 1994.

[5] Ioana Chişu, K.A. Biro, I.A. Viorel, H.C. Hedeşiu, R.C. Ciorba, "On the synchronous reluctance machine rotor geometry", in *Proc. Electromotion 1999*, Vol. 1, pp. 161-166.

[6] B.J. Chalmers, A. Williamson, *AC machines electromagnetics and design*, John Wiley and Sons Inc., New York (1991).